Energy Efficiency of Video Broadcasting Services in LTE Heterogeneous Networks

Dragan Rastovac*, Chadi Khirallah†, Dejan Vukobratović*, John Thompson†
*Dept. of Power, Electronics and Communication Engineering, University of Novi Sad, Serbia
†School of Engineering, The University of Edinburgh, Edinburgh, UK

***Abstract*—Significant part of the expected surge for mobile video delivery in upcoming years will be accommodated through video multicasting/broadcasting services. In particular, the evolution of 3GPP Multimedia Broadcasting/Multicasting Service (eMBMS) is a promising recent step in preparing 4G infrastructure for massive video broadcast. However, 3GPP currently considers only macro-cellular approaches for eMBMS delivery while at the same time, the evolved UMTS Radio Access Network (E-UTRAN) is evolving towards small cells deployment following Heterogeneous Networks (HetNets) concepts. In this paper, we consider energy consumption within E-UTRAN as a consequence of transition of video broadcasting service delivery from macro-cellular to HetNets layouts. We provide energy efficiency evaluation for different HetNets deployment scenarios under varying system parameters and compare it to the baseline macro-cellular eMBMS scenario.**

I. Introduction

Recent estimates predict dramatic increase in the amount of video traffic requested by mobile end-users of the upcoming fourth generation (4G) cellular networks. For example, Cisco VNI claims the 18-fold increase of mobile data traffic by 2016, which will set video streaming as dominant traffic category in mobile cellular networks [1]. As a response, 3GPP has increased activities in the domain of standardization of new or updated mobile video services targeting efficient solutions for the evolving 3GPP Long-Term Evolution - Advanced (LTE-A) cellular standard [2]. Former activities on unicast streaming are now mainly targeted towards Dynamic Adaptive HTTP Streaming (DASH) service [3], while broadcast/multicast services are addressed by new and evolved Multimedia Broadcast/Multicast Service (eMBMS) proposals [4].

The eMBMS is recently presented with two proposed transmission schemes [5]. In the first one, single-cell (SC-eMBMS) transmission, each base station (eNB) independently maintains the eMBMS service delivery following user feedback on channel conditions and dynamic selection of the suitable physical layer (PHY) transmission mode. In the second one, multi-cell or so called single frequency network (SFN-eMBMS) transmission, macro eNBs coordinate their transmission to cover the network with the same physical signal, where a fixed PHY scheme adapted to the worst case service users is applied.

With the ongoing evolution from macro-cellular to Heterogeneous Networks (HetNets) layout, the potential for offering higher-quality video services increases. The introduction of small cells aims at increasing the quality and predictability of user channels for the price of additional investments in infrastructure. Thus HetNets based evolved UMTS Radio Access Network (E-UTRAN) offers novel opportunities for enhancements in mobile video delivery services including eMBMS through, e.g., service "offloading" from macro cells to small cells or dynamic power control ("cell-zooming") of small cells. On the other hand, E-UTRAN energy efficiency becomes major concern as introduction of small cells places additional burden on E-UTRAN power consumption.

In this paper, we investigate the impact of deployment of HetNets based E-UTRAN on eMBMS service delivery in LTE-A. We build upon our recent work on energy evaluation of SC and SFN eMBMS service discussed in [6]. Using recently developed energy consumption models for different classes of base stations in E-UTRAN, we evaluate and compare the total E-UTRAN energy consumption for provisioning of fixed-rate eMBMS service channels over various E-UTRAN configurations including the traditional macro-cellular layout. The SC-eMBMS service is assumed where service traffic is offloaded to small cells whenever a mobile user equipment (UE) that consumes the service experiences better (i.e., higher average rates) connection via a neighbouring small cell eNBs compared to the connection towards macro eNB. Our results demonstrate that introduction of small cells provides improved E-UTRAN energy efficiency in terms of the total system energy required to deliver a fixed bit-rate services.

The paper is organized as follows. Sec. II provides necessary background for the paper. In Sec. III, we present the system model and methodology for evaluation of average service data rates at UEs serviced within the cell. The same section includes energy consumption models of different eNB classes and discussion on total E-UTRAN energy consumption. Simulation results that compare energy efficiency of various E-UTRAN configurations are presented in Sec. IV. The paper is concluded in Sec. V.

II. Background

A. Video Broadcasting Services Over LTE/LTE-A

3GPP defines two major categories for video delivery services over LTE: the unicast services such as recently popular 3GPP DASH solution targeting unicast media streaming to small groups of users [3], and the 3GPP eMBMS suitable for broadcasting the same video content to a large number of users over a common radio channel [4].

Starting from Release 6, 3GPP standards present architectural solutions for MBMS [5]. In Release 8, the enhanced

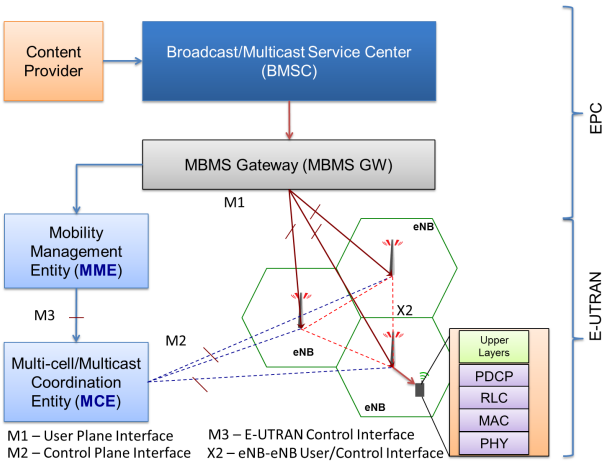

Fig. 1. 3GPP eMBMS System Architecture.

MBMS (eMBMS) design is presented via two different architectural solutions [8]. The first one, single-cell (SC-eMBMS) transmission, overcomes pre-LTE MBMS shortcomings by allowing user feedback on channel conditions and dynamic selection of the suitable modulation and coding (MC) PHY mode. The advantage of this scheme is dynamic adaptation to current distribution of users in the cell. Furthermore, in terms of energy efficiency, the SC-eMBMS service can be switched-off in the cells with no active service. The second one, multi-cell or so called single frequency network (SFN-eMBMS) transmission, represents a coordinated effort of macro eNBs to cover the network with the same physical signal, where a fixed MC scheme adapted to match the worst-case edge-user requirements is applied. SFN-eMBMS results in increased achievable rates at the cell edge. In contrast to SC-eMBMS, SFN-eMBMS is fixed and designed in advance and does not depend on the user distribution over the cells [5].

The eMBMS system architecture is illustrated in Fig. 1 [9]. For SC-eMBMS, which is in focus of this paper, a similar architecture as for the standard LTE unicast service with the eMBMS service gateway (MBMS GW) and the Mobility Management Entity (MME) is used. SFN-eMBMS requires additional coordination within single frequency network of eNBs, which is maintained by Multi-cell multicast Coordination Entity (MCE). Service-level entity called Broadcast/Multicast Service Center (BMSC) maintains service activation and session management between service users and the content provider.

B. 3GPP LTE/LTE-A RAN Protocols

Once the IP packetized video content reaches eNB, it is delivered to the mobile UE via E-UTRAN radio-link connections [8]. The set of protocol responsible for IP flow downlink delivery at the eNB/UE interface, illustrated at the UE in Fig. 1, are presented in more detail in Fig. 2.

Following header compression and ciphering in Packet Data Conversion Protocol (PDCP), PDCP encapsulated IP packets (IP/PDCP) are delivered to the Radio Link Control (RLC) layer. The RLC layer segments or concatenates IP/PDCP packets into RLC packets to exactly match the MAC frame size requirements. The MAC frame size is determined by the MAC Scheduler to fit the physical layer (PHY) transport block (TB) size, which finally depends on the PHY MC scheme selected at the eNB. Informally, the flow of IP packets at the upper layers is rearranged to fit into the stream of PHY TB containers [11].

TABLE I
CQI VALUES AND THE CORRESPONDING TB SIZES.

CQI index	**modulation**	**code rate**	**bits per symbol**	**SINR** (dB)	**TBS** (bits)
$0-3$	No Tx	-	-	< -1.25	0
4	QPSK	0.3	0.6016	-0.94	384
5	QPSK	0.44	0.8770	1.09	576
6	QPSK	0.59	1.1758	2.97	768
7	16QAM	0.37	1.4766	5.31	960
8	16QAM	0.48	1.9141	6.72	1152
9	16QAM	0.6	2.4063	8.75	1536
10	64QAM	0.45	2.7305	10.47	1920
11	64QAM	0.55	3.3223	12.34	2304
12	64QAM	0.65	3.9023	14.37	2688
13	64QAM	0.75	4.5234	15.94	3072
14	64QAM	0.85	5.1152	17.81	3456
15	64QAM	0.93	5.5547	20.31	3840

The PHY TB represents a PHY packet whose size (TBS) within a single transmission time interval (TTI) depends on the MC scheme selected by the MAC Scheduler and the amount of PHY resource blocks (RBs) allocated to the service delivery. The PHY RB represents a unit of time-frequency resources: 0.5 ms time duration ($\frac{1}{2}$ TTI) and 12 OFDM carriers (180 kHz) of bandwidth. PHY RBs are always allocated in pairs, thus the PHY TBS depends on the number N_{RBP} of RB pairs (RBPs), 1 RBP = 180 kHz $\times$ 1 TTI (see Table I, TBS column for the case $N_{RBP} = 6$, i.e., a Category 1 LTE user).

For SFN-eMBMS, the PHY MC scheme is fixed across the whole SFN network throughout the service delivery. For SC-eMBMS, it can be changed dynamically based on the UE feedback in the form of Channel Quality Indicator (CQI) values and each eNB may select its own appropriate PHY parameters. For more details on the LTE E-UTRAN protocols, we refer the reader to [10][11].

III. Energy Efficiency of eMBMS in E-UTRAN

This paper builds upon our recent energy efficiency evaluation of SC and SFN eMBMS service in macro-cellular LTE layouts discussed in [6]. Thus we reuse the same system model and methodology for average service rate calculation, extended in this paper to include deployment of small cells, more precisely, the micro and pico eNBs. For completeness, we shortly provide the rate and energy evaluation approach used in this paper which follows the approach in [6].

A. The System Model

The LTE-A system model we observe is represented by a macro-cellular site that combines 19 macro-cell eNBs arranged in two tiers around a central eNB. We focus on the central

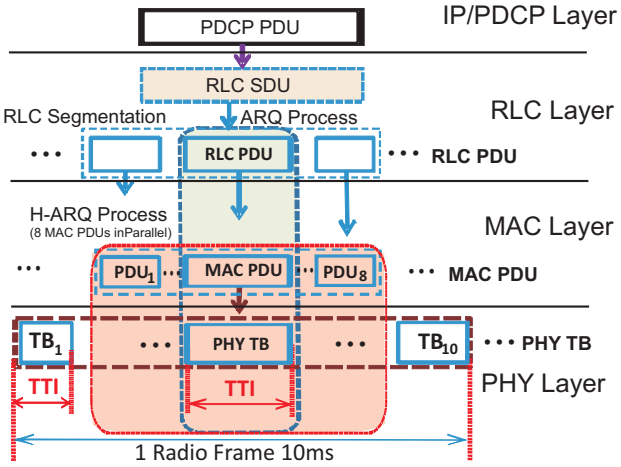

Fig. 2. eNB DL packet flow from IP to PHY layer.

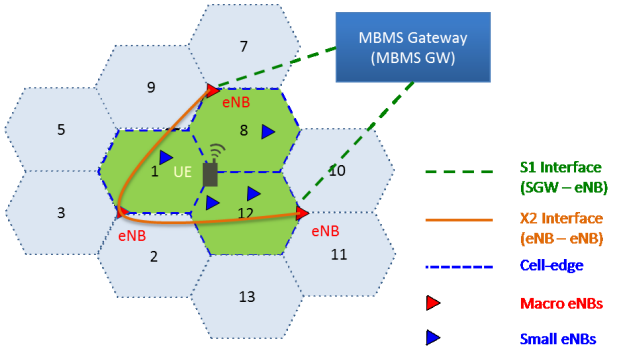

Fig. 3. Part of the LTE-A HetNets layout.

cell and randomly deploy additional small cells into the cell area. We assume a given number of micro and pico eNBs is randomly placed according to Poisson point process. Each class of eNBs (macro, micro and pico) is allocated a separate and disjoint set of PHY RBs (the same approach can be used if small cells reuse the same set of PHY RBs as the macro-cellular network). eMBMS service is provided over a fixed set of allocated PHY RBs using SC-eMBMS. Fig. 3 illustrates part of the HetNets layout.

For a UE placed at a distance d from the eNB, the average SINR at the UE is [8]:

$$SINR(d) = P_{TX} + G_{TX} + G_{RX} - \\ - N - I - S(d) - PL(d) - PNL, \quad (1)$$

where P_{TX} is the eNB transmission power; G_{TX} and G_{RX} are the eNB and the UE antenna gains (including 3GPP defined horizontal and vertical antenna patterns for macro eNBs); N and I are the noise and the ICI power from all the interfering eNBs at the UE location; PNL is the wall penetration loss for signals received at indoor UEs; and finally, S and PL are the shadowing loss and the pathloss in dB measured at different UE positions using shadowing variances and path loss models defined in Table II following [8].

The ICI factor I depends on the received signal power from

TABLE II
LTE/LTE-A PARAMETERS AND SYSTEM ASSUMPTIONS

Parameter	Value
Inter site distance (ISD)	500 m (3GPP Case 1)
Traffic model	Downlink full buffer
Duplexing mode	FDD
System bandwidth	2 x 40 MHz (LTE-A)
eMBMS service allocation	25%
Subcarrier spacing	7.5 kHz
Number of usable data RBs/TTI	100 RBPs per 10 MHz
OFDMA useful symb duration	0.133 ms
Number of OFDMA symb/frame	6 per subframe
Number of RBPs per TTI	100 RBPs
MBMS control overhead	10%
Transmission scheme	SISO
Frame duration	10 ms
Carrier frequency	2.0GHz
System layout	multi-cell (19 macro-cells)
Pathloss	eNB-UE 3GPP model
Penetration loss (PNL)	20dB
Shadowing	Shadow fading: Log normal Std deviation: eNB-UE:8dB
Terminal speed	3km/h
Max Tx power	eNB:46dBm/sector
Max Antenna gain	eNB:14dBi, UE:0dBi
Antenna height	eNB:25m, UE:1.5m
Noise figure	UE:7dB
Max. HARQ retransmissions	3

all the eNBs except the strongest one. Due to separate bands applied for macro, micro and pico eNBs, only eNBs from the same class interfere each other.

B. Average Downlink Transmission Rate

Based on the average SINR calculated at the UE position, we model the small-scale channel variations using Finite State Markov Chain (FSMC) channel models [12]. The FSMC model applied here represents the evolution of CQI values the UE would report during the sequence of consecutive time (TTI) intervals. We apply slowly-varying frequency-flat Rayleigh fading FSMC model [13], customized so that it "embeds" the existing LTE division of SINR axis into the FSMC model in order to obtain the time-dynamics and asymptotic steady-state behaviour of *CQI states* (Table I, SINR column) [6]. The resulting FSMC model represents PHY TB transmission process that underlies the multimedia IP services over LTE E-UTRAN.

Using the FSMC model, one can easily derive the set $\boldsymbol{\pi} = \{\pi_1, \pi_2, \ldots, \pi_{N_{CQI}}\}$ of steady state probabilities of CQI states [13], where N_{CQI} is the number of CQI states. While in the i-th CQI state, the average data rate achievable at the UE equals:

$$R_i = \frac{TBS(i) \cdot N_{RBP}}{TTI}(1 - BLER(i)), \quad (2)$$

where $TBS(i)$ is the PHY TB information capacity (in bits) used while the channel is in the CQI state i (Table I, TBS column) and $BLER(i)$ is the average BLER of the i-th state (e.g., 10% PHY TB loss rate [10]). Finally, we obtain the average rate $R_{avg}(d)$ of PHY TB data delivery over the eNB-UE interface for the UE placed at the distance d from the

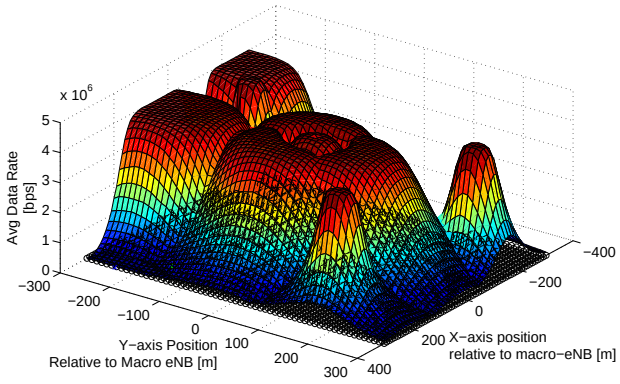

Fig. 4. Average data rates for a HetNets deployment example.

eNB:

$$R_{avg}(d) = \boldsymbol{\pi} \cdot \boldsymbol{R}^T, \quad (3)$$

where $\boldsymbol{R} = \{R_1, R_2, \ldots, R_{N_{CQI}}\}$. Note that the rates calculated using (3) correspond to average rates achievable using unicast transmission, where the eNB continuously adapts the MC scheme to the UE reported CQI values. For broadcast transmission, where the eNB applies fixed MC scheme corresponding to the CQI value s, the values in $\boldsymbol{R}$ are obtained as follows: $R_i = R_s$, for all $i \geq s$, and $R_i = 0$ otherwise. As an example, Figure 4 presents average rate achieved at different points of the macro-cellular region with two micro and three pico base stations deployed randomly in the cell are. For each UE position, the strongest eNB is selected and the remaining eNBs are regarded as interferers, under restriction that macro and small cells operate in different frequency bands.

C. Heterogeneous Base Station Energy Consumption

To investigate the energy efficiency of SC-eMBMS in HetNets based a E-UTRAN, we first define a suitable macro, micro and pico eNB power consumption models, from which we directly obtain the energy costs for a given fixed rate eMBMS service. In general, eNB power models consist of dynamic and static components. While the dynamic part varies with the eNB average transmission power and the instantaneous traffic load, the static part (or zero-load) is independent of these parameters and represents the power consumption in equipment such as the transceiver (base-band and radio), climate control (cooling sections) and interfaces [14][15].

For power consumption evaluation, several models are available. Here, we use macro and micro eNB power consumption model from [14] and pico eNB power consumption model from [16]. For example, for the macro eNB, we use the power consumption model proposed in [14]:

$$P_M = N_{PA} \cdot \left(\frac{P_{TX}}{\mu_{PA} + P_{SP}} \right) \cdot (1 + C_C) \cdot (1 + C_{PSBB}), \quad (4)$$

where the above equation holds per sector of the macro eNB. The following values are considered (UMTS1 Model from [14]): the number of power amplifiers per sector $N_{PA} = 1$; total eNB transmission power $P_{TX} = 40$W; power amplifier efficiency $\mu_{PA} = 0.15$; signal processing power dissipation $P_{SP} = 73.5$W; and cooling and battery supply losses are $C_C = 0.28$ and $C_{PSBB} = 0.11$, respectively. For the micro eNB, we use the same source and exactly the same parameters used therein [14] (Sec. 2.4, eqs. (3) and (4)), while for the pico eNB, we use the model and parameters from [16].

IV. Simulation Results

In this section, we present our simulation methodology and provide results on energy consumption of various LTE HetNets configurations for eMBMS service delivery. We focus on the system layout described in Sec. III-A, more precisely, on the central macro eNB and the circular area of radius R_C. The radius R_C is selected as the maximum radius of the circle centered in the macro eNB such that none of the points within the circle receives higher SINR from any other but central macro eNB. Within the circle, we randomly place mobile users according to Poisson point process of density $\lambda = \frac{N_{UE}}{R_C^2 \pi}$. Similarly, we randomly place N_μ and N_p micro and pico cells in the circle. Following the eNB and UE placement, we assume the UE selects the point of connection to be the eNB (macro or small) that provides the highest average SINR.

In each simulation run, we aim to calculate the amount of frequency resources that every eNB has to allocate in order to be able to offer an average eMBMS service rate of R[kbps]. In other words, we assume that each eNB (macro or small) is notified on all the UEs it serves and their respective SINR values. From this information the eNB extracts the worst-case user, and using eqs. (2) and (3) as a function of N_{RBP}, calculates the minimum amount of frequency resources $N_{RBP}^{(eNB)}$, i.e., PHY RBPs, it has to allocate so that the worst-case user average rate R_{min}^{eNB} exceeds the service rate R. Finally, we take this information into account for the total energy consumption calculation. Namely, the total power eNB invested in the eMBMS is obtained by pondering the dynamic component of the total power expressions with the amount (fraction) of resources used for eMBMS service at each serving eNB.

Fig. 5 illustrates the results obtained for the macro-only scenario. The figure illustrates the total energy consumption in the cell for a fixed-rate eMBMS service provisioning as a function of the user density (N_{UE}). The results demonstrate approximately linear growth of required energy investments with the user density, propelled mostly by the fact that larger user density drives some users to the cell edge area with increasing probability. Increasing the service rate increases the rate of the power consumption increase with the increase of the user density.

Fig. 6 focuses on the R=256kbps eMBMS service and in addition to macro-only scenario, we randomly deploy $N_\mu = \{1, 5, 10\}$ micro base stations. From the results in the figure, we clearly see the benefit of increasing micro-cellular deployment density for energy efficiency while delivering fixed-rate service across the cell. For the case of large number of micro-cells, the cell coverage with the requested data rate is already sufficiently high resulting in the energy costs that remain nearly constant with the increase of the user density.

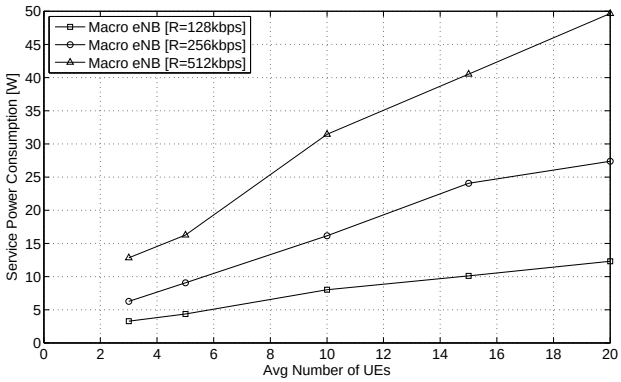

Fig. 5. Average eMBMS service power consumption for macro cellular configuration as a function of UE density and service data rates.

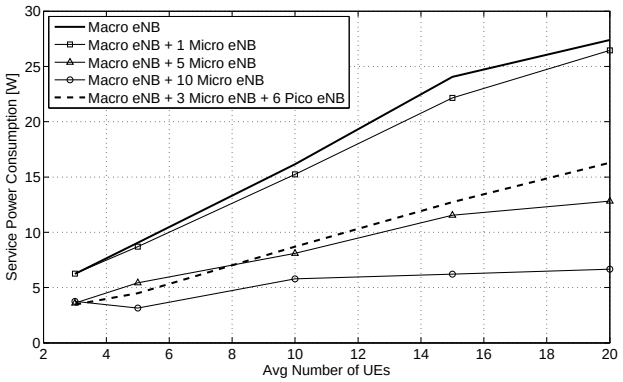

Fig. 6. Average eMBMS service power consumption for different HetNets configuration as a function of UE density (R=256kbps).

Finally, in the figure, we also include the case of combined macro/pico deployment. We illustrate the scenario where, apart from macro eNB, we randomly place $N_\mu = 3$ micro eNBs and $N_\mu = 6$ pico eNBs. The resulting energy costs for fixed rate R=256kbps eMBMS service turns out to be similar as for the case of $N_\mu = 5$ micro eNBs. Thus certain energy costs per service channel may be obtained using different HetNets configurations and providing optimal solution for a given service requirements is part of our ongoing efforts.

V. Conclusions

In this paper, we analyzed the energy efficiency of future E-UTRAN HetNets deployments for provisioning of eMBMS based video broadcasting services. We applied standard 3GPP defined path loss models for various macro and small eNBs overlaid by a more detailed FSMC-based model of instantaneous channel behaviour, for the purpose of the average rate estimation at each UE position. In parallel, for energy consumption estimation we used recently proposed energy consumption models for various types of macro and small eNBs. Finally, the two models provided us detailed energy efficiency analysis for video service provisioning in future LTE HetNets environment. The preliminary results demonstrate that the versatility provided by HetNets environment could be exploited towards the search of the energy efficient E-UTRAN layouts.

References

[1] Cisco Visual Networking Index, http://www.cisco.com/en/US/netsol/ /ns827/networking_solutions_sub_solution.html

[2] F. Gabin, M. Kampmann, T. Lohmar, and C. Priddle, "3GPP Mobile Multimedia Streaming Standards," *IEEE Signal Processing Magazine*, Vol. 27(6), pp. 134–138, 2010.

[3] ETSI TS 26.247 v11.0.0 (Rel. 11), Transparent end-to-end Packet-switched Streaming Service (PSS); Progressive Download and Dynamic Adaptive Streaming over HTTP (3GP-DASH), 2012.

[4] ETSI TS 26.346 v10.1.0 (Rel. 10), UMTS-Multimedia Broadcast/Multicast Service (MBMS); Protocols and Codecs, 2011.

[5] M. Gruber and D. Zeler, "Multimedia Broadcast Multicast Service: New Transmission Scheme and Related Challenges," *IEEE Comm. Magazine,* Vol. 49, No. 12, pp. 176-181, Dec. 2011.

[6] C. Khirallah, D. Vukobratovic, and J. Thompson: "Bandwidth and Energy Efficiency of Video Broadcasting Services over LTE/LTE-A," IEEE WCNC 2013, Shanghai, China, April 2013.

[7] O. Oyman, J. Foerster, T. Y-J. Tcha, S-C. Lee, "Towards Enhanced Mobile Video Services over WiMAX and LTE," *IEEE Comm. Magazine,* Vol. 48, No. 8, pp. 68-76, Aug. 2010.

[8] 3GPP TR 36.913 V8.0.1 (Release 8), Requirements for further advancements for E-UTRA, March 2009.

[9] ETSI TS 36.440 v11.0.0 (Rel. 11), Evolved Universal Terrestrial Radio Access Network (E-UTRAN); General aspects and principles for interfaces supporting Multimedia Broadcast Multicast Service (MBMS) within E-UTRAN, 2012.

[10] A. Larmo, M. Lindstrom, M. Meyer, G. Pelletier, J. Torsner, H. Wiemann: "The LTE Link-Layer Design," *IEEE Comms. Mag.*, Vol. 47, No. 4, pp: 52-59, April 2009.

[11] H. Holma and A. Toskala, LTE for UMTS : Evolution to LTE-Advanced, Second Edition, Wiley, 2011.

[12] P. Sadeghi, R. A. Kennedy, P. B. Rapajic and R. Shams, "Finite-State Markov Modeling of Fading Channels: A Survey of Principles and Applications," *IEEE Signal Process. Mag.,* Vol 57, pp. 57-80, Sept. 2008.

[13] Q. Zhang, and S. Kassam: "Finite-State Markov Model for Rayleigh Fading Channels," *IEEE Transactions on Communications,* Vol. 47, No. 11, pp. 1688-1692, November 1999.

[14] Arnold, O., Richter, F., Fettweis, G., Blume, O.: "Power consumption modeling of different base station types in heterogeneous cellular networks" IEEE Future Network and Mobile Summit, 2010.

[15] C. Khirallah, J. S. Thompson, and H. Rashvand, "Energy and Cost Impact of Relay and Femtocell Deployments in LTE-Advanced," *IET Comm.,* Vol. 5, No. 18, pp. 2617–2628, Dec. 2011.

[16] Tombaz, S., Monti, P., Wang, K., Vastberg, A., Forzati, M., and Zander, J.: "Impact of backhauling power consumption on the deployment of heterogeneous mobile networks" IEEE GLOBECOM 2011, Dec. 2011.